

The exotic H_3^{2+} ion in a strong magnetic field. Linear configuration.

A. V. Turbiner,^{*} J. C. López Vieyra,[†] and N. L. Guevara[‡]

*Instituto de Ciencias Nucleares, Universidad Nacional Autónoma de México,
Apartado Postal 70-543, 04510 México, D.F., Mexico*

Abstract

An accurate study of the lowest $1\sigma_g$ and the low-lying excited $1\sigma_u$, $1\pi_{u,g}$, $1\delta_{g,u}$ electronic states of the exotic molecular ion H_3^{2+} in linear configuration parallel to a magnetic field is carried out. The magnetic field ranges from 10^{10} G up to 4.414×10^{13} G where non-relativistic considerations are justified. The variational method is exploited and the *same* trial function is used for different magnetic fields. It is shown that the states of positive z -parity $1\sigma_g, 1\pi_u, 1\delta_g$ are bound states of the H_3^{2+} exotic ion for all magnetic fields studied. We also demonstrate that for magnetic fields $B \gtrsim 2.35 \times 10^{12}$ G the potential energy surface well corresponding to the $1\sigma_g$ state contains at least one longitudinal vibrational state. It is also shown that the negative z -parity states $1\sigma_u, 1\pi_g, 1\delta_u$, are purely repulsive in the whole range of magnetic fields studied, $B = 10^{10} - 4.414 \times 10^{13}$ G.

PACS numbers: 31.15.Pf, 31.10.+z, 32.60.+i, 97.10.Ld

^{*}On leave of absence from the Institute for Theoretical and Experimental Physics, Moscow 117259, Russia;

Electronic address: turbiner@nuclecu.unam.mx

[†]Electronic address: vieyra@nuclecu.unam.mx

[‡]Electronic address: nicolais@nuclecu.unam.mx

I. INTRODUCTION

Recently, it was announced that in a sufficiently strong magnetic field $B \gtrsim 10^{11} G$ three protons situated on the magnetic line can be bound by one electron forming the exotic molecular ion H_3^{2+} in linear configuration [1]. A major feature of this configuration is that with a magnetic field growth the system becomes more and more bound (binding energy grows), and more and more compact (equilibrium distance decreases). Later it was shown that this exotic ion H_3^{2+} in linear configuration becomes even the most stable one-electron system with smallest total energy for magnetic fields $B \gtrsim 10^{13} G$ [2]. A recent study has demonstrated that the H_3^{2+} molecular ion can also exist in a certain spatial configuration – the protons form an equilateral triangle while a magnetic field is directed perpendicular to it [3]. The goal of this article is to make a detailed quantitative study of the ground state and the lowest excited states of the H_3^{2+} -ion in a linear configuration for $B = 10^{10} - 4.414 \times 10^{13} G$, which was announced in [1]. In particular, this is the first study of the lowest excited states of the H_3^{2+} ion.

Atomic units are used throughout ($\hbar=m_e=e=1$), although energies are expressed in Rydbergs (Ry). The magnetic field B is given in a.u. with $B_0 = 2.35 \times 10^9 G$.

II. GENERALITIES

We study the system of three protons and one electron (*pppe*) placed in a uniform constant magnetic field. It is assumed that the protons are infinitely heavy (Born-Oppenheimer approximation of zero order) and that they are situated along the magnetic field direction forming a linear chain. The Hamiltonian which describes this system when the magnetic field is directed along the z -axis, $\mathbf{B} = (0, 0, B)$ is written as

$$\mathcal{H} = \hat{p}^2 + \frac{2}{R_+} + \frac{2}{R_-} + \frac{2}{R_+ + R_-} - \frac{2}{r_1} - \frac{2}{r_2} - \frac{2}{r_3} + (\hat{p}\mathcal{A} + \mathcal{A}\hat{p}) + \mathcal{A}^2, \quad (1)$$

(see Fig. 1 for the geometrical setting and notations), where $\hat{p} = -i\nabla$ is the momentum, \mathcal{A} is a vector potential which corresponds to the magnetic field \mathbf{B} . It is chosen in the symmetric gauge,

$$\mathcal{A} = \frac{B}{2}(-y, x, 0).$$

Hence, the total energy E_T of the H_3^{2+} -ion is defined as the total electronic energy plus the Coulomb energy of proton repulsion. The binding energy is defined as the affinity of the

system to form a bound state with respect to the system when the electron and the three protons are infinitely separated, $E_b = B - E_T$. There are two dissociation processes: one of them has in the final state a hydrogen atom, $H_3^{2+} \rightarrow H + 2p$ while the other one has a H_2^+ molecular ion, $H_3^{2+} \rightarrow H_2^+ + p$. Therefore, the first dissociation energy is defined as the affinity of the system to form a bound state having two protons at infinity, $E_{d_{\text{atom}}} = E_H - E_T$, where E_H is the total energy of the hydrogen atom in a magnetic field B . While the second dissociation energy is defined as an affinity to form a bound state having one proton at infinity, $E_{d_{\text{ion}}} = E_{H_2^+} - E_T$, where $E_{H_2^+}$ is the total energy of the hydrogen molecular ion H_2^+ in a magnetic field B . A contribution coming from the spin degrees of freedom is neglected.

The problem we study is characterized by two integrals of motion: (i) the operator of the z -component of the angular momentum (projection of the angular momentum on the magnetic field direction) giving rise to the magnetic quantum number m and (ii) the spatial parity operator $P(\vec{r} \rightarrow -\vec{r})$ which has eigenvalue $p = \pm 1$. Hence, any eigenstate has two explicit quantum numbers assigned: the magnetic quantum number m and the parity p . Therefore the space of eigenstates is split into subspaces (sectors) with each of them characterized by definite values of m and p . It is worth to note that the Hamiltonian (1) is also invariant with respect to $z \rightarrow -z$. Therefore, in general one can classify the eigenstates using the quantum number $\sigma = \pm 1$ for positive/negative z -parity instead of p . However, this classification is related with the above described - there exists a relation between the quantum numbers corresponding to the z -parity and the spatial parity:

$$p = \sigma(-1)^m .$$

To classify eigenstates we follow the convention widely accepted in quantum chemistry using the quantum numbers m and p . In particular, the notation for the states that we are going to use is similar to that introduced for H_2^+ -ion in parallel configuration [5] and is based on the following: the first number corresponds to the number of excitation - "principal quantum number", e.g. the number 1 is assigned to the ground state (lowest state), then Greek letters σ, π, δ correspond to the states with $m = 0, -1, -2$, respectively, with subscript g/u (gerade/ungerade) describing positive/negative parity p .

The excited states which we plan to study are the lowest states (of the type of the ground state) of the sectors with different magnetic quantum numbers m and p . It is quite obvious from a physical point of view that the ground state of a sector with $m > 0$ always has larger

total energy than those with $m \leq 0$. For this reason we restrict our consideration to the states with $m = 0, -1, -2$.

Conservation of the z -component of the angular momentum implies that the electronic wave function (in cylindrical coordinates (ρ, φ, z)) can be written as

$$\Psi = e^{im\varphi} \rho^{|m|} \psi_m , \quad (2)$$

where m is the magnetic quantum number. If we gauge rotate the Hamiltonian (1) with a factor from (2), it takes the form

$$\mathcal{H}_m = e^{-im\varphi} \rho^{-|m|} \mathcal{H} e^{im\varphi} \rho^{|m|} = \hat{p}_m^2 + \frac{2}{R_+} + \frac{2}{R_-} + \frac{2}{R_+ + R_-} - \frac{2}{r_1} - \frac{2}{r_2} - \frac{2}{r_3} + mB + \frac{B^2 \rho^2}{4} , \quad (3)$$

where

$$\hat{p}_m = e^{-im\varphi} \rho^{-|m|} \hat{p} e^{im\varphi} \rho^{|m|} ,$$

is the gauge rotated momentum (covariant momentum) and ψ_m are the eigenfunctions. The constant term mB describes the linear Zeeman effect splitting. In principle this term can be absorbed into the definition of the total energy. The representation (3) is rather convenient since each Hamiltonian for fixed m describes the family of eigenstates with quantum number m and can be treated independently of the states with m' different from m . Now the Hamiltonian (3) has only the invariance corresponding to the spatial parity conservation.

As a method to explore the problem we use the variational procedure. The recipe of choice of trial functions is based on physical arguments and is described in full generality in [6], where we address the reader. The ground state trial function for fixed m and p is chosen in the form

$$\psi_m^{(trial)} = A_1 \psi_1 + A_2 \psi_2 + A_3 \psi_3 + A_4 \psi_4 + A_5 \psi_5 + A_6 \psi_6 , \quad (4)$$

with $\psi_1 \dots \psi_6$ given by

$$\psi_1 = \begin{cases} e^{-\alpha_1(r_1+r_2+r_3)}e^{-B\beta_1\rho^2/4}, & \text{if } \sigma = +1 \\ 0, & \text{if } \sigma = -1 \end{cases} \quad (5a)$$

$$\psi_2 = \begin{cases} (e^{-\alpha_2r_1} + e^{-\alpha_2r_2} + e^{-\alpha_2r_3})e^{-B\beta_2\rho^2/4}, & \text{if } \sigma = +1 \\ 0, & \text{if } \sigma = -1 \end{cases} \quad (5b)$$

$$\psi_3 = \begin{cases} (e^{-\alpha_3(r_1+r_2)} + e^{-\alpha_3(r_1+r_3)} + e^{-\alpha_3(r_2+r_3)})e^{-B\beta_3\rho^2/4}, & \text{if } \sigma = +1 \\ 0, & \text{if } \sigma = -1 \end{cases} \quad (5c)$$

$$\psi_4 = (e^{-\alpha_4r_1-\alpha_5r_2} + \sigma e^{-\alpha_5r_1-\alpha_4r_2} + e^{-\alpha_5r_1-\alpha_4r_3} + \sigma e^{-\alpha_4r_1-\alpha_5r_3} + e^{-\alpha_4r_2-\alpha_5r_3} + \sigma e^{-\alpha_5r_2-\alpha_4r_3})e^{-B\beta_4\rho^2/4}, \quad (5d)$$

$$\psi_5 = \begin{cases} (e^{-\alpha_6(r_1+r_2)-\alpha_7r_3} + e^{-\alpha_6(r_1+r_3)-\alpha_7r_2} + e^{-\alpha_6(r_2+r_3)-\alpha_7r_1})e^{-B\beta_5\rho^2/4}, & \text{if } \sigma = +1 \\ 0, & \text{if } \sigma = -1 \end{cases} \quad (5e)$$

$$\psi_6 = (e^{-\alpha_8r_1-\alpha_9r_2-\alpha_{10}r_3} + \sigma e^{-\alpha_9r_1-\alpha_8r_2-\alpha_{10}r_3} + e^{-\alpha_{10}r_1-\alpha_8r_2-\alpha_9r_3} + \sigma e^{-\alpha_8r_1-\alpha_{10}r_2-\alpha_9r_3} + e^{-\alpha_9r_1-\alpha_{10}r_2-\alpha_8r_3} + \sigma e^{-\alpha_{10}r_1-\alpha_9r_2-\alpha_8r_3})e^{-B\beta_6\rho^2/4}, \quad (5f)$$

where for the sake of convenience of a representation we use the quantum number σ . The functions $\psi_1 \dots \psi_6$ are S_3 invariant with respect to the permutations of the identical protons and $\sigma = \pm 1$ corresponds to the symmetric (antisymmetric) trial functions. It is clear that the functions $\psi_1 \dots \psi_6$ are also eigenfunctions of the z -parity operator ($p_z\psi_i = \sigma\psi_i$, $i = 1 \dots 6$).

In Eqs. (5), $A_{1,\dots,6}$ and $\alpha_{1,\dots,10}, \beta_{1,\dots,6}$, as well as the internuclear distances R_{\pm} (see Fig. 1) are variational parameters [13]. The total number of parameters is 23 for the symmetric case ($\sigma = +1$) and 10 for the antisymmetric case ($\sigma = -1$) [14]. The functions $\psi_{1\dots 6}$ carry a certain physical meaning. The function ψ_1 (ψ_2) describes a coherent (incoherent) interaction of the electron with the protons. The functions ψ_3, ψ_4 describe a coherent interaction of the electron with two protons (it may be called as H_2^+ type interaction). In a certain sense it corresponds to the interaction of H_2^+ with a proton. The function ψ_5 represents an interaction of the electron with all three charged centers of the type $(H_2^+ - H\text{-atom})$ -mixture. Finally the function ψ_6 is a nonlinear interpolation of the functions $\psi_1 \dots \psi_6$.

Calculations were performed using the minimization package MINUIT from CERN-LIB. Numerical integrations were carried out with a relative accuracy of $\sim 10^{-11}$ by use of the adaptive D01FCF routine from NAG-LIB. All calculations were performed on a dual PC with

two Xeon processors of 2.8 GHz each. Every particular calculation of a given eigenstate at fixed magnetic field including minimization has taken several hours of CPU time. However, when the variational parameters are found it takes a few seconds of CPU time to calculate the variational energy.

It is necessary to mention two technical difficulties we encountered. Calculation of two-dimensional integrals with high accuracy which appeared in the problem has required a development of a very sophisticated numerical technique. It was created a ‘dynamical partitioning’ of the domain of integration, which depends on the values of the variational parameters (see e.g. [4]). The domain partitioning was changed with a change of the parameters. Sometimes the number of sub-domains in particular integration was around 20. Another technical problem is related with a very complicated profile of the variational energy as function of the variational parameters which is characterized by many local minima, saddle points and valleys. Localization of the global minimum numerically of such a complicated function with high accuracy is a difficult technical problem which becomes even more difficult in the case of twenty or more variational parameters. Examining the physical relevance of trial functions allows us to avoid spurious minima. The parameters obtained in (4) at every step of minimization were always examined from the physical point of view. Such considerations are always something of an art.

III. RESULTS

A. $m = 0$

The $m = 0$ subspace consists of two subspaces, $p = 1$ (even states) and $p = -1$ (odd states).

1. $1\sigma_g$ state ($p = 1$)

The state $1\sigma_g$ is the global ground state of the exotic H_3^{2+} -ion. Its eigenfunction has no nodes (Perron theorem). For this state our variational trial function (4) with $m = 0, p = 1$ depends effectively on twenty-two parameters (see footnote [13]). In comparison with the trial function used in the first studies [1, 2] we have added two extra ansatz, ψ_4 and ψ_5 . As it was mentioned above, the search for the global minimum numerically with high accuracy in

the case of so many variational parameters is a difficult technical task. We use a sophisticated strategy for localizing the minimum. As a first step we minimize ansatz by ansatz, then we take a superposition of two ansatz, then three ansatz etc. An essential element of the strategy is to impose a (natural) condition that the variational parameters change smoothly as a function of the magnetic field B . The above-mentioned strategy allowed us to improve our previous results for the ground state reported in [2] on total and binding energies, and also on the lowest vibrational energies. The qualitative results remain unchanged (see below).

The performed variational calculations indicate clearly to the existence of a minimum in the potential energy surface $E_T(R_+, R_-)$ of the (*pppe*) system for magnetic fields ranging $B = 10^{10} - 4.414 \times 10^{13}$ G. The minimum in the total energy always corresponds to the situation when $R_+ = R_- \equiv R_{eq}^{H_3^{2+}}$ confirming the qualitative symmetry arguments. Table I shows the results for the total E_T and binding energies E_b , as well as the internuclear equilibrium distance $R_{eq}^{H_3^{2+}}$ for the ground state $1\sigma_g$ calculated with the trial function (4) and with the trial function used in our previous studies (Eq.(4) with $A_4 = A_5 = 0$) [1, 2]. Thus, we predict that the exotic H_3^{2+} ion can exist even in a larger domain of magnetic field strengths as reported in [1, 2]. We confirm a general statement that with an increase of the magnetic field strength the total energies increase, the system becomes more bound (binding energies increase) and more compact (the internuclear equilibrium distance decreases).

In general, for all one-electron systems (in linear configuration) the binding energy increases asymptotically as $\propto \log^2 B$ for strong magnetic fields (for a discussion about the case of the hydrogen atom see e.g. [7]). In the domain we study ($B = 10^{10} - 4.414 \times 10^{13}$ G) the rate of increase of binding energy for H_3^{2+} is slightly larger than the corresponding rates for the H atom and for the H_2^+ ion (see [4, 5]). As a result, for magnetic fields $B \gtrsim 4 \times 10^{10}$ G the H_3^{2+} ion becomes more bound than the H atom, and for magnetic fields $B \gtrsim 3 \times 10^{13}$ G, H_3^{2+} becomes the most bound (having the lowest total energy and the largest binding energy) among the one-electron systems H , H_2^+ , H_3^{2+} .

An straightforward analysis of the internuclear equilibrium distances shows that in the domain $B = 10^{10} - 4.414 \times 10^{13}$ G the rate of decrease of the internuclear equilibrium distance for the H_3^{2+} ion is also larger than the corresponding rate for the H_2^+ ion ($R_{eq}^{H_3^{2+}}$ decreases in ~ 20 times, while $R_{eq}^{H_2^+}$ decreases in ~ 10 times when we go from $B = 10^{10}$ G to 4.414×10^{13} G). Making a comparison between H_3^{2+} and H_2^+ one can see that the internuclear

equilibrium distance for H_3^{2+} is always larger than that for H_2^+ . The internuclear distances converge to each other as the magnetic field increases: $R_{eq}^{H_3^{2+}} = 0.110$ a.u., while $R_{eq}^{H_2^+} = 0.102$ a.u. at $B = 4.414 \times 10^{13}$ G (see [4, 5]).

Another important feature of the system is the behavior of its dissociation as a function of the magnetic field. There are two dissociation processes: $H_3^{2+} \rightarrow H_2^+ + p$ (i) and $H_3^{2+} \rightarrow H + 2p$ (ii). Table I shows the dissociation energies corresponding to these processes $E_{d_{ion}} = E_{H_2^+} - E_T$ and $E_{d_{atom}} = E_H - E_T$, respectively, for different magnetic fields. Let us consider the first process (i). A negative dissociation energy $E_{d_{ion}}$ indicates that the ion H_3^{2+} is unstable towards the decay $H_3^{2+} \rightarrow H_2^+ + p$. In particular, for $B \gtrsim 10^{10}$ G $E_{d_{ion}}$ is negative and decreases with a magnetic field growth reaching the minimum at $B \sim 10000$ a.u. Then, for further magnetic field increase the dissociation energy (which is still negative) starts to increase monotonously. Eventually, for a magnetic field $B \simeq 3 \times 10^{13}$ G the dissociation energy becomes zero which means $E_T = E_{H_2^+}$ and then starts to be positive. It implies that the ion H_3^{2+} becomes more bound than H_2^+ and, in fact, this ion becomes the most stable one electron system. The above described behavior for the dissociation $H_3^{2+} \rightarrow H_2^+ + p$ also indicates that, for a broad domain of magnetic fields, there exist two different values of the magnetic field for which we have the same dissociation energy $E_{d_{ion}}$.

The situation is different for the second dissociation process (ii), $H_3^{2+} \rightarrow H + 2p$. The dissociation energy $E_{d_{atom}}$ increases monotonously in all the range of studied magnetic fields. In the domain $10^{10} - 4 \times 10^{10}$ G the dissociation energy $E_{d_{atom}}$ is negative and it indicates that the ion H_3^{2+} is unstable towards the decay $H_3^{2+} \rightarrow H + 2p$. For magnetic fields $B \gtrsim 4 \times 10^{10}$ G the dissociation energy is positive and the ion H_3^{2+} is more bound than the H atom. For comparison the dissociation energies $E_{d_{atom-ion}}$ for the process $H_2^+ \rightarrow H + p$ are also shown in Table I [15]. For magnetic fields $B \gtrsim 10^{11}$ G, the dissociation energy $E_{d_{atom}}$ for the dissociation $H_3^{2+} \rightarrow H + 2p$ is smaller than the corresponding dissociation energy for $H_2^+ \rightarrow H + p$ except for the domain $B > 10000$ a.u.

The improvement in the total energy obtained using the trial function (4) in comparison to the results based on the reduced trial function (4) ($A_4 = A_5 = 0$) [4, 5] is the order of $\sim (1 - 5) \times 10^{-3}$ Ry for the whole range of magnetic fields studied. It represents a relative improvement of $\sim 0.01\% - 0.05\%$ in the binding energies (see Table I).

We should notice that in our previous studies [1, 2] a different definition of the magnetic field atomic unit was used for unit conversion ($B_0 = 2.3505 \times 10^9$ G). It leads to a relative

difference in the total energies of order of 10^{-4} . It should be taken into account when a comparison of the results in [1, 2] and the present results is made.

We show in Fig. 2 the behavior of the variational parameters of the trial function (4) as a function of the magnetic field strength. In general, the behavior of the parameters is rather smooth and *very* slowly-changing, even though the magnetic field changes by several orders of magnitude. In our opinion such a behavior of the parameters of our trial function (4) reflects the level of adequacy (or, in other words, indicates the quality) of the trial function. In practice, the parameters can be approximated by the splines method and then can be used to study magnetic field strengths other than those presented here.

a. Potential Energy Surfaces, Vibrational Energies. We carried out a detailed accurate study of the electronic potential surface $E_T(R_+, R_-)$ around the minimum and also along the valleys and around the barriers which ensure the existence of bound states. It allowed us to estimate accurately the (lowest) longitudinal vibrational energies.

Let us first proceed to a description of the valleys of potential energy surfaces. Every potential surface is characterized by two valleys originated from the minimum. Those valleys are symmetric with respect to the bisectriz $R_+ = R_-$. Therefore it is sufficient to study a single valley and in further considerations we will be focused on one of the valleys which is almost horizontal. In Fig. 4 the valleys in the (R_+, R_-) plane and the profile along a valley are shown for different magnetic fields. Every profile is characterized by a minimum which corresponds to the equilibrium ($R_+ = R_- = R_{eq}$) and a potential barrier. The height of the potential barrier is defined with respect to the energy corresponding to the equilibrium position (minimum) $\Delta E_T = E_T^{max} - E_T^{min}$. The asymptotics of the profile corresponds to decay of the system to $H_2^+ + p$, for example, when $R_+ \rightarrow \infty$ (and $R_- \rightarrow R_{eq}^{H_2^+}$) or similarly $R_- \rightarrow \infty$ (and $R_+ \rightarrow R_{eq}^{H_2^+}$).

The pattern of the valley in the (R_+, R_-) plane exhibits a rather complicated behavior (see Fig. 4, where the behavior near minimum is displayed in amplified form). For example, for the horizontal valley the R_- firstly grows reaching some maximum, then decreases reaching a minimum and after that increases approaching to asymptotics in R_+ from below. A similar picture holds for all magnetic fields studied. We do not think that this type of behavior is an artifact of insufficient accuracy of our calculations. In principle, the energy profile curve allows us to estimate the lifetime of the system with respect to the decay $H_3^{2+} \rightarrow H_2^+ + p$ for magnetic fields $10^{10} \text{ G} \lesssim B \lesssim 4 \times 10^{13} \text{ G}$. However, such study is beyond the scope of the

present analysis.

Table II shows the values of the height of the potential barrier ($\Delta E_T = E_T^{max} - E_T^{min}$) along the valley of total energy and the position of the top of the energy barrier. From this table one can see that for the domain of magnetic fields $B = 10^{11} - 4.414 \times 10^{13}$ G the height of the potential barrier increases dramatically from ~ 0.01 Ry up to ~ 5 Ry, respectively[16].

Now let us proceed to a calculation of the lowest longitudinal vibrational state. The method we use is based on the harmonic approximation of the potential around the minimum. All necessary definitions to perform the analysis are similar to those which are used to study the vibrational states of linear triatomic molecules and can be found in standard textbooks (see, for example, [9]). Following the settings of Fig.1, we find easily the normal coordinates: $R_s = \frac{1}{\sqrt{2}}(R_+ + R_-)$ (it corresponds to the “symmetric” normal mode), and $R_a = \frac{1}{\sqrt{2}}(R_+ - R_-)$ (it corresponds to the “anti-symmetric” normal mode). The lowest vibrational energy is then calculated as $E_0^{vib} = E_0^s + E_0^a$, where $E_0^s = \sqrt{\frac{k_s}{m_p}}$ and $E_0^a = \sqrt{\frac{3k_a}{m_p}}$ are the lowest “symmetric” and “anti-symmetric” vibrational energies respectively, $m_p = 1836.15$ is the proton mass measured in units of the electron mass, and k_s, k_a are the curvatures taken in a.u. near equilibrium for the symmetric and antisymmetric modes, respectively.

The results for the lowest vibrational energies E_0^{vib} for different magnetic fields are shown in Table II. These results indicate that with a magnetic field growth the form of the potential well around the minimum becomes sharper and the lowest vibrational energies increase drastically growing from ~ 0.1 Ry at $B = 10^{11}$ G up to ~ 2 Ry at $B = 4.414 \times 10^{13}$ G [17]. Then, we can conclude that the energy well contains at least one vibrational state for magnetic fields $B \gtrsim 1000$ a.u.

b. Electronic distributions. The equilibrium configuration is characterized by a one-peak electronic distribution centered around the middle proton, being drastically shrunk in the direction transverse to the magnetic field as compared with the longitudinal direction (see Fig. 5, it is worth to note that the different scales are used for the x and z axes). This one-peak form of the electronic distribution for equilibrium position is found for all magnetic fields studied. Also the electronic cloud has always a needle-like form. When the system is out of equilibrium, the electronic distributions show the appearance of a pronounced shoulder which follows the position of the more distant proton, reducing its height as the system approaches to the decaying configuration, where the electronic density

TABLE I: Total E_T and binding E_b energies, internuclear equilibrium distances R_{eq} and dissociation energies $E_{d_{ion}} = E_{H_2^+} - E_T$ ($H_3^{2+} \rightarrow H_2^+ + p$) and $E_{d_{atom}} = E_H - E_T$ ($H_3^{2+} \rightarrow H + 2p$) for the state $1\sigma_g$. Dissociation energies $E_{d_{atom-ion}} = E_H - E_{H_2^+}$ ($H_2^+ \rightarrow H + p$) are shown for comparison. Results marked by asterisks (*) correspond to a trial function (4) with $A_{4,5} = 0$ (four Ansatz function, Turbinder and López-Vieyra, unpublished 2003).

B	E_T (Ry)	E_b (Ry)	R_{eq} (a.u.)	$E_{d_{ion}}$ (Ry)	$E_{d_{atom}}$ (Ry)	$E_{d_{atom-ion}}$ (Ry)	
10^{10} G	1.8424	2.4129	2.072	-0.7519	-0.2020	0.5500	present
	1.8438	2.4116	2.061				(*)
10 a.u.	6.6084	3.3916	1.431	-0.9581	-0.1039	0.8542	present
	6.6094	3.3906	1.429				(*)
10^{11} G	36.4297	6.1234	0.801	-1.3865	0.4105	1.7966	present
	36.4327	6.1205	0.799				(*)
100 a.u.	91.3611	8.6389	0.579	-1.6521	1.0596	2.7117	present
	91.3655	8.6345	0.578				(*)
10^{12} G	410.3739	15.1580	0.345	-1.9845	3.2427	5.2272	present
	410.3762	15.1558	0.345				(*)
1000 a.u.	979.2171	20.7829	0.259	-1.9956	5.4615	7.4571	present
	979.2206	20.7794	0.259				(*)
10^{13} G	4220.9286	34.3905	0.166	-1.3634	11.8395	13.2029	present
	4220.9320	34.3872	0.166				(*)
10000 a.u.	9954.5918	45.4082	0.130	-0.3890	17.4532	17.8422	present
	9954.5972	45.4028	0.130				(*)
4.414×10^{13} G	18727.7475	55.2312	0.110	0.7294	22.7305	22.0010	present
	18727.7521	55.2267	0.110				(*)

rearranges to mimic the electronic distribution of the H_2^+ ion. Nothing especial seems to occur for the configuration near the top of the potential barrier. To illustrate the above-mentioned features we present on Fig. 5 the normalized electronic density distributions $\Psi^2(x, y = 0, z)/\int \Psi^2(x, y, z)d\vec{r}$ and the corresponding contour distribution for the magnetic field $B = 10000$ a.u. for different positions of the system H_3^{2+} along the valley in potential surface in R_+, R_- . In this presentation we always keep the central proton at $z = 0$. The following points along the valley are chosen: (a) the equilibrium position, $R_+ = R_- = 0.13$ a.u., (b) a point between positions of minimum and maximum, $R_+ = 0.23$ a.u., (c) a point close to the maximum, $R_+ = 0.35$ a.u. (maximum is around $R_+ \simeq 0.36$ a.u. – see Table II) and (d) a point on the asymptotic part of the valley where one of the protons is practically detached from the system.

TABLE II: Energies of the lowest longitudinal vibrational states (E_0^{vib}), height of the potential barrier ($\Delta E_T = E_T^{max} - E_T^{min}$) and position of the maximum ($R_+(E_{max}), R_-(E_{max})$) in the valley corresponding to the ground state $1\sigma_g$ of the H_3^{2+} molecular ion in a magnetic field. Results marked by asterisks * are interpolated values of the height of the barrier using a cubic polynomial fit in the variable $\log(1+B^2)$ and the position of the maximum using a fit of the form $R_{\pm}(E_{max}, B) = 1/P_2^{\pm}$, where P_2^{\pm} is a quadratic polynomial in the variable $\log(1+B^2)$.

B	E_0^{vib} (Ry)	ΔE_T (Ry)	$R_+(E_{max})$ (a.u.)	$R_-(E_{max})$ (a.u.)
10^{11} G	0.0951	0.0101	0.94	0.758
100 a.u.	0.154	0.1007*	0.77 *	0.517 *
10^{12} G	0.338	0.267	0.58	0.294
1000 a.u.	0.530	0.581 *	0.50*	0.221 *
10^{13} G	1.088	1.895	0.40	0.147
10000 a.u.	1.594	3.339*	0.36 *	0.118 *
4.414×10^{13} G	2.078	4.815	0.33	0.101

2. $1\sigma_u$ state ($p = -1$)

We have performed a detailed study for the state $1\sigma_u$ of the H_3^{2+} ion in symmetric configuration $R_+ = R_- \equiv R$ in the domain of magnetic fields $B = 10^{10} - 4.414 \times 10^{13}$ G. The calculations were carried out using the trial function (4) with $m = 0$ and $p = -1$ corresponding to a state of negative z -parity ($\sigma = -1$). For a broad domain of internuclear distances R the electronic potential curve $E_T = E_T(R)$ shows no indication of the existence of a minimum. Hence, it is natural to conclude that this state is a purely repulsive state for $B = 10^{10} - 4.414 \times 10^{13}$ G. It means that the molecular ion H_3^{2+} does not exist in the $1\sigma_u$ state as a bound state.

B. $m = -1$

The subspace consists of two subspaces, $p = 1$ (even states) and $p = -1$ (odd states).

1. $1\pi_u$ state ($p = -1$)

We study the $1\pi_u$ state of ($pppe$) system in symmetric configuration $R_+ = R_- \equiv R$. The trial function (4) is taken with $m = -1$ and $p = -1$ (which implies $\sigma = 1$). The variational calculations indicate that the potential energy curve $E_T = E_T(R)$ has clear minimum for magnetic fields $B = 2.35 \times 10^{10} \text{ G} - 4.414 \times 10^{13} \text{ G}$. It manifests that H_3^{2+} ion exists in $1\pi_u$ state. The results are presented in Table III. Similar to the state $1\sigma_g$ the binding energy of the $1\pi_u$ state grows steadily with a magnetic field increase while the equilibrium distance shrinks in a quite drastic manner. For small magnetic fields the state $1\pi_u$ is more extended than $1\sigma_g$. The equilibrium distance R_{eq} for $1\pi_u$ is much larger than this distance for the $1\sigma_g$ state, as for large magnetic fields these equilibrium distances become comparable. Among the $m = -1$ states the state $1\pi_u$ has the smallest total energy. A comparison with the corresponding energy of the $1\pi_u$ state of H_2^+ (cf. Table VII in [5]) shows that the energy of the $1\pi_u$ state of H_3^{2+} is always larger for $B = 2.35 \times 10^{10} \text{ G} - 4.414 \times 10^{13} \text{ G}$.

Transition energy from the $1\sigma_g$ state to the $1\pi_u$ state, $E_{1\pi_u} - E_{1\sigma_g}$ is easily calculated by taking data from Tables I and III. In the whole range of magnetic fields studied the transition energy increases monotonically with the magnetic field growth as expected (see Fig. 3).

In Fig. 6(a) a plot of the normalized electronic density distribution $\Psi^2(x, y = 0, z) / \int \Psi^2(x, y, z) d\vec{r}$ for the $1\pi_u$ excited state in a magnetic field of $B = 10000 \text{ a.u.}$ is shown. By looking at the corresponding contour distribution it is evident that the electronic cloud has a torus-like axially-symmetric form with respect to the z -axis. The radial size of the torus[18] decreases with a magnetic field increase. A similar qualitative behavior of the electronic density distribution is observed for different magnetic fields .

2. $1\pi_g$ state ($p = 1$)

We have performed a detailed study for the state $1\pi_g$ of the H_3^{2+} ion in symmetric configuration $R_+ = R_- \equiv R$ in the domain of magnetic fields $B = 10^{10} - 4.414 \times 10^{13} \text{ G}$. The calculations were carried out using the trial function (4) with $m = -1$ and $p = 1$ corresponding to a state of negative z -parity ($\sigma = -1$). For a broad domain of internuclear distances R the electronic potential curve $E_T = E_T(R)$ shows no indication of the existence

TABLE III: Total E_T , binding E_b energies and equilibrium distance R_{eq} for the excited state $1\pi_u$.

B	E_T (Ry)	E_b (Ry)	R_{eq} (a.u.)
10 a.u.	7.9289	2.0711	2.413
10^{11} G	38.6589	3.8943	1.238
100 a.u.	94.3927	5.6073	0.869
10^{12} G	415.3661	10.1658	0.497
1000 a.u.	985.7952	14.2048	0.366
10^{13} G	4231.0542	24.2649	0.226
10000 a.u.	9967.3669	32.6331	0.174
4.414×10^{13} G	18742.7564	40.2223	0.145

of a minimum. Hence, it is natural to conclude that this state is a purely repulsive state for $B = 10^{10} - 4.414 \times 10^{13}$ G. It means that the molecular ion H_3^{2+} does not exist in the $1\pi_g$ state as a bound state.

C. $m = -2$

The subspace consists of two subspaces, $p = 1$ (even states) and $p = -1$ (odd states).

1. $1\delta_g$ state ($p = 1$)

We study the $1\delta_g$ state of (*pppe*) system in symmetric configuration $R_+ = R_- \equiv R$. The trial function (4) is taken with $m = -2$ and $p = 1$ (which implies $\sigma = 1$). The variational calculations indicate that the potential energy curve $E_T = E_T(R)$ has clear minimum for magnetic fields $B = 2.35 \times 10^{10} \text{ G} - 4.414 \times 10^{13} \text{ G}$. It manifests that H_3^{2+} ion exists in $1\delta_g$ state. The results are presented in Table IV. Similar to the states $1\sigma_g$ and $1\pi_u$ the binding energy of the $1\delta_g$ state grows steadily with a magnetic field increase while the equilibrium distance shrinks in a quite drastic manner. For small magnetic fields the equilibrium distance $R = R_{eq}$ for $1\delta_g$ is much larger than this distance for the $1\sigma_g$ and $1\pi_u$ state, as for large magnetic fields all three equilibrium distances become comparable. Among the $m = -2$ states the state $1\delta_g$ has the smallest total energy. A comparison with the corresponding energy of the $1\delta_g$ state of H_2^+ (cf. Table IX in [5]) shows that the energy of the $1\delta_g$ state of H_3^{2+} is always larger for $B = 2.35 \times 10^{10} \text{ G} - 4.414 \times 10^{13} \text{ G}$.

Transition energies from the $1\pi_u$ state to the $1\delta_g$ state $E_{1\delta_g} - E_{1\pi_u}$ can be easily calculated from Tables III and IV showing a monotonically increasing behavior in all range of magnetic fields studied (see Fig. 3). It is worth to note that the transition energy from $1\pi_u$ state to the $1\delta_g$ state is always smaller than the transition energy from $1\sigma_g$ state to the $1\pi_u$ state.

In Fig. 6(b) a plot of the normalized electronic density distribution $\Psi^2(x, y = 0, z) / \int \Psi^2(x, y, z) d\vec{r}$ for the $1\delta_g$ excited state in a magnetic field of $B = 10000 \text{ a.u.}$ is shown. Similar to the case of the $1\pi_u$ state, the electronic cloud for the $1\delta_g$ state has a torus-like axially symmetric form with respect to the magnetic field line (z -axis). It is worth to note that the radial size of this torus-like form of the electronic distribution for the $1\delta_g$ state is larger than for the $1\pi_u$ state.

2. $1\delta_u$ state ($p = -1$)

We have performed a detailed study for the state $1\delta_u$ of the H_3^{2+} ion in symmetric configuration $R_+ = R_- \equiv R$ in the domain of magnetic fields $B = 10^{10} - 4.414 \times 10^{13} \text{ G}$.

TABLE IV: Total E_T , binding E_b energies and equilibrium distance R_{eq} for the state $1\delta_g$.

B	E_T (Ry)	E_b (Ry)	R_{eq} (a.u.)
10 a.u.	8.3644	1.6356	3.214
10^{11} G	39.4450	3.1082	1.548
100 a.u.	95.4919	4.5081	1.070
10^{12} G	417.2496	8.2823	0.601
1000 a.u.	988.3293	11.6707	0.437
10^{13} G	4235.0826	20.2366	0.266
10000 a.u.	9972.5387	27.4613	0.202
4.414×10^{13} G	18748.9067	34.0720	0.167

The calculations were carried out using the trial function (4) with $m = -2$ and $p = -1$ corresponding to a state of negative z -parity ($\sigma = -1$). For a broad domain of internuclear distances R the electronic potential curve $E_T = E_T(R)$ shows no indication to the existence of a minimum. Hence, one can conclude that this state is a purely repulsive state for $B = 10^{10} - 4.414 \times 10^{13}$ G. It means that the molecular ion H_3^{2+} does not exist in the $1\delta_u$ state as a bound state.

IV. CONCLUSION

We have carried out an accurate, non-relativistic calculation in the Born-Oppenheimer approximation for the low-lying states of the H_3^{2+} molecular ion in the linear parallel configuration placed in a constant uniform magnetic fields ranging from $B = 10^{10}$ G to $B = 4.414 \times 10^{13}$ G. Similar to the study of the H_2^+ ion [5] we used a variational method with a simple (and unique), several parametric trial function inspired by the underlying physics of the problem for all range of magnetic fields studied. Our trial function can be easily analyzed and in contrast to other approaches our results can be easily reproduced and checked. Also the trial function (4) can be easily modified to explore other excited states. We showed that the exotic ion H_3^{2+} exists in the states of positive z -parity $1\sigma_g$, $1\pi_u$ and $1\delta_g$, and does not exist in the states of negative z -parity $1\sigma_u$, $1\pi_g$ and $1\delta_u$ $B = 2.35 \times 10^{10}$ G – 4.414×10^{13} G. The present study complements our previous study of the ground state performed in [1] and

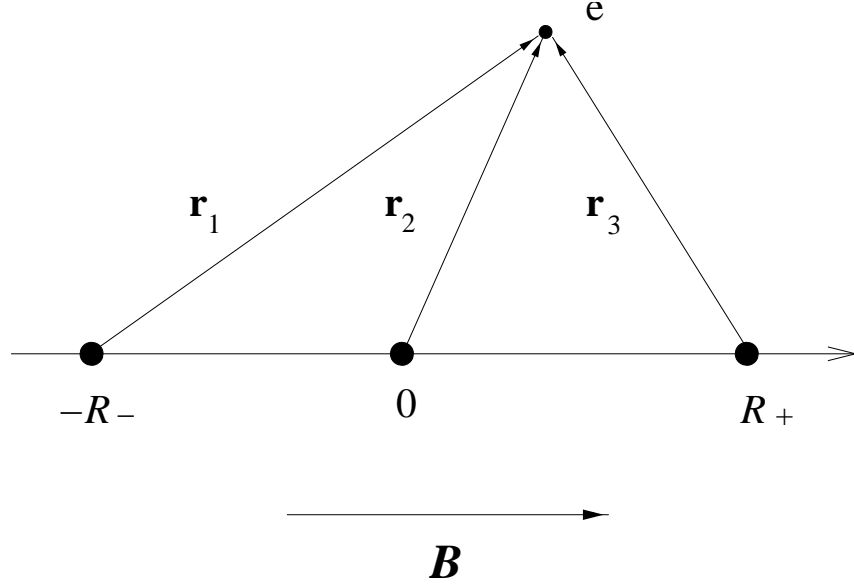


FIG. 1: Geometrical setting for the H_3^{2+} ion placed in a magnetic field directed along the z -axis. The protons (marked by bullets) are situated on the z -line at distances R_{\pm} from the central proton which is placed at the origin.

[2].

It is evident that the state $1\sigma_g$ having no nodes is the global ground state of the system ($pppe$) (if exists) for all magnetic fields (Perron theorem). It is clear that this statement remains valid in general, when even the states other than studied are taken into account. We show for the ($pppe$) system in state of positive z -parity the electronic potential surface $E_T(R_+, R_-)$ always develops a minimum corresponding to the symmetric configuration $R_+ = R_-$, when the protons are situated on equal distances between each other. The domain of existence of the H_3^{2+} ion is slightly extended in comparison to the previous studies [1, 2] to be $B = 10^{10} - 4.414 \times 10^{13} G$. For the case of excited states of the positive z -parity ($1\pi_u, 1\delta_g$) we also find a minimum in the potential surface for a similar domain of magnetic fields $B = 2.35 \times 10^{10} - 4.414 \times 10^{13} G$. A common feature for these bound states is that the total and binding energies grow with an increase in the magnetic field strength, while the internuclear equilibrium distances reduce drastically.

For fixed magnetic field the energies of the positive z -parity states are ordered following the value of the magnetic quantum number m ,

$$E_T^{1\sigma_g} < E_T^{1\pi_u} < E_T^{1\delta_g} ,$$

as well as the equilibrium internuclear distances

$$R_{eq}^{1\sigma_g} < R_{eq}^{1\pi_u} < R_{eq}^{1\delta_g} .$$

This order holds also in the whole domain of magnetic fields studied (see Tables I, III, and IV). The same time for the fixed magnetic field the binding energies of the states of positive z -parity are reduced slow with excitation (see Tables I,III,IV). It gives us a chance to expect that other states of the positive z -parity can exist for some magnetic fields.

For the $1\sigma_g$ state we studied the electronic potential energy surfaces for different magnetic fields. All those surfaces in addition to the minimum corresponding to the bound state (*pppe*) display two symmetric valleys running from the minimum to infinity corresponding to the “path” of the decay $H_3^{2+} \rightarrow H_2^+ + p$. For magnetic fields $B \lesssim 3 \times 10^{13}$ G the H_3^{2+} exotic ion is unstable towards the decay $H_3^{2+} \rightarrow H_2^+ + p$.

Our analysis of the lowest longitudinal vibrational state and the height of the potential barrier (see Table II) allow us to conclude that for magnetic fields $B \gtrsim 2.35 \times 10^{12}$ G, the well of the potential energy surface of the ground state $1\sigma_g$ contains at least one vibrational state.

Since for magnetic fields $B \gtrsim 3 \times 10^{13}$ G the H_3^{2+} ion is the most stable one-electron system, this study can be of considerable importance, in particular, in the construction of adequate atomic-molecular models of the neutron star atmospheres, where typical magnetic fields are $B \simeq 10^{12}$ G or higher. A recent application of the present approach, although for larger magnetic fields where relativistic corrections start to be of a certain importance (for a discussion see e.g. [10]), were used to construct a model of the atmosphere of the isolated neutron star 1E1207.4-5209 (see [11]) which is based on the assumption that the main component of such atmosphere is nothing but the exotic molecular ion H_3^{2+} [12].

Acknowledgments

This work was supported in part by CONACyT grants **25427-E** and **36600-E** (Mexico). The authors are grateful to H. Olivares for a help in numerical calculations.

- [1] A.V. Turbiner, J.C. López Vieyra, U. Solis H. *Pis'ma v ZhETF* **69**, 800-805 (1999)
JETP Letters **69**, 844-850 (1999) (English Translation), (astro-ph/9809298)
- [2] J.C. López Vieyra and A.V. Turbiner, *Phys. Rev.* **A62**, 022510 (2000)
- [3] A.V. Turbiner and J.-C. Lopez Vieyra, *Phys. Rev.* **A66**, 023409 (2002)
- [4] A.V. Turbiner and J.C. Lopez-Vieyra, *Phys. Rev.* **A68**, 012504 (2003) (astro-ph/0212463)
- [5] A.V. Turbiner and J.C. Lopez-Vieyra, *Phys. Rev.* **A69**, 053413 (2004) (astro-ph/0310849)
- [6] A.V. Turbiner, *ZhETF* **79**, 1719 (1980); *Soviet Phys.-JETP* **52**, 868 (1980) (English Translation); *Usp. Fiz. Nauk.* **144**, 35 (1984); *Sov. Phys. – Uspekhi* **27**, 668 (1984) (English Translation); *Yad. Fiz.* **46**, 204 (1987); *Sov. Journ. of Nucl. Phys.* **46**, 125 (1987) (English Translation); Doctor of Sciences Thesis, ITEP, Moscow, 1989 (unpublished), ‘Analytic Methods in Strong Coupling Regime (large perturbation) in Quantum Mechanics’
- [7] L. D. Landau and E. M. Lifshitz, *Quantum Mechanics*, Pergamon Press (Oxford - New York - Toronto - Sydney - Paris - Frankfurt), 1977
- [8] A. Y. Potekhin and A. V. Turbiner, *Phys. Rev.* **A63**, 065402 (2001)
- [9] H. Goldstein, ‘*Classical mechanics*’, Addison-Wesley, 1980. 2d ed.
- [10] D. Lai, E. Salpeter and S. L. Shapiro, *Phys. Rev.* **A45**, 4832 (1992)
- [11] D. Sanwal et al., *ApJL*, **574**, L61 (2002) (astro-ph/0206195)
- [12] A.V. Turbiner and J.C. López Vieyra, astro-ph/0404290
- [13] Due to the normalization of the wave function one of the coefficients A should be kept fixed. Usually, we put $A_1 = 1$
- [14] We always assume following symmetry arguments and check it afterwards numerically that the optimal configuration corresponds to $R_+ = R_-$. Effectively it reduces the number of variational parameters.
- [15] the total energies for the Hydrogen atom were calculated using the 7-parametric variational trial function used in [8] but with $B_0 = 2.35 \times 10^9$ G

- [16] A comparison of the present results for the height of the potential barrier, with those reported in [2] shows an increasing loss of accuracy of the latter with increasing magnetic field (their ratio varies between $\sim 0.2 - 0.8$ in the domain of magnetic fields $10^{11} - 4.414 \times 10^{13}$ G respectively).
- [17] A comparison of the present results for the lowest vibrational energies with our previous results [2] shows that there is a difference in a factor ~ 2 . It appears due to a mistake in normalization of the normal modes used in [2] (cf. Table I therein).
- [18] We can defined the radius of the torus-like form as the distance from the origin of the z -axis to the point of maximal probability.

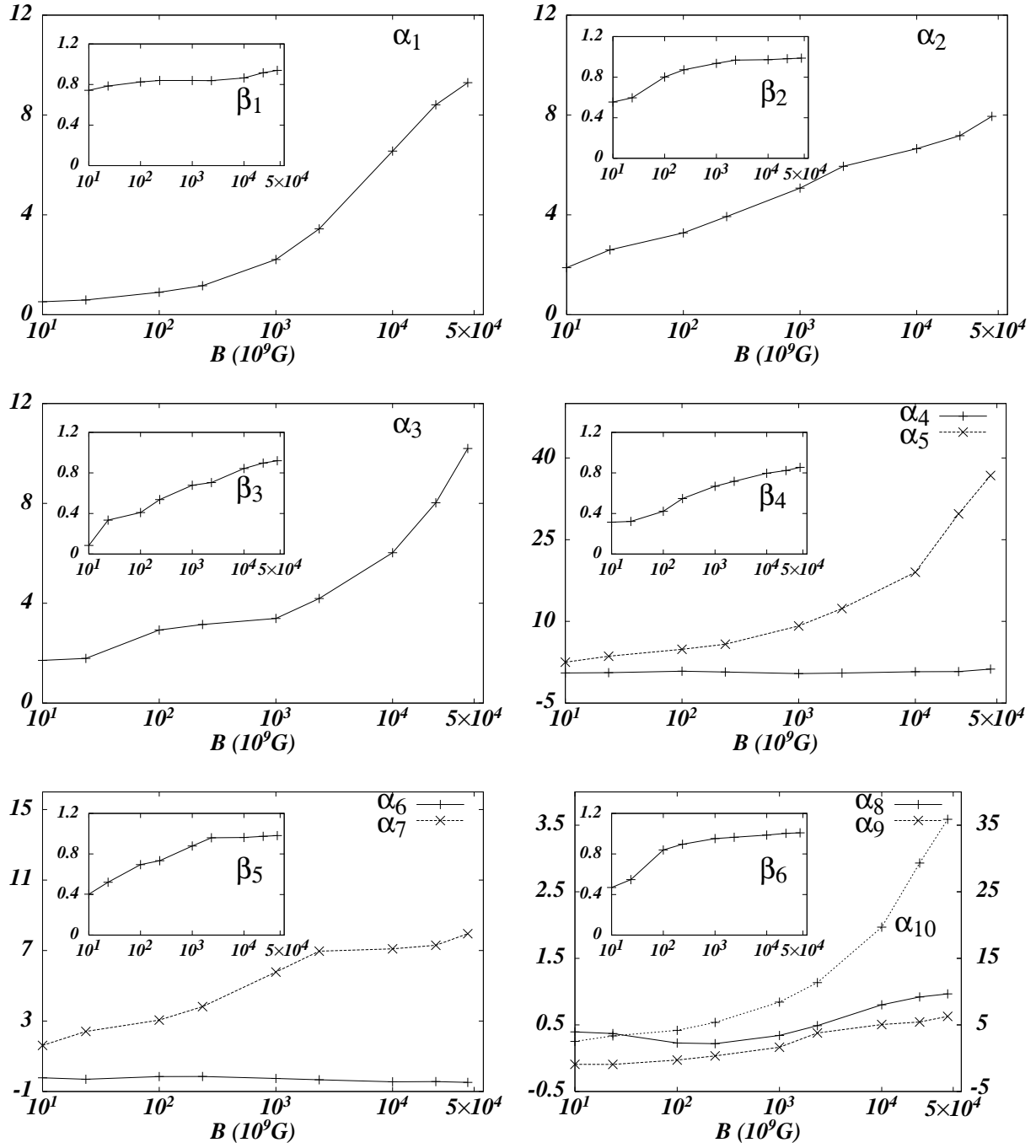


FIG. 2: Variational parameters of the trial function (5) (see text) for the state $1\sigma_g$ at the equilibrium position as a function of the magnetic field strength B . Parameters $\alpha_{1...10}$ are of dimension $[a.u.]^{-1}$ and the parameters $\beta_{1...6}$ are dimensionless. The parameter A_1 is placed equal to 1. In the figure where the parameters $\alpha_{8,9,10}$ are shown the right scale corresponds to the parameter α_{10} .

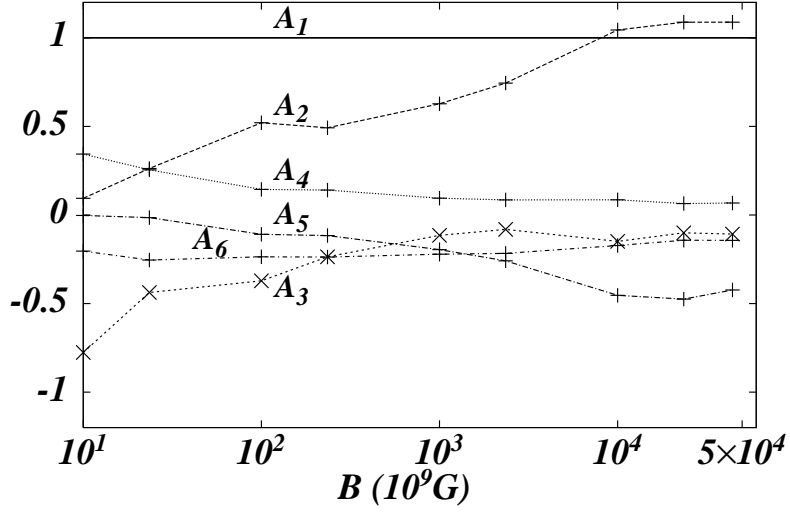


FIG. 2: Continuation

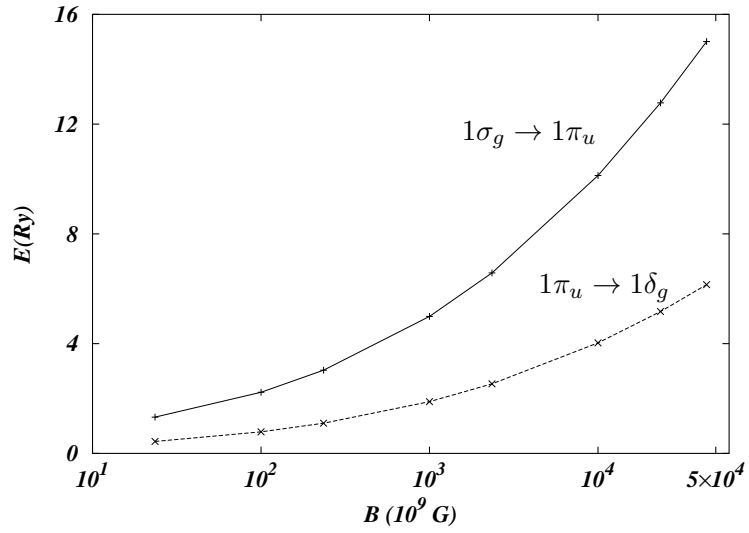


FIG. 3: Transition energies between the lowest three states of the H_3^{2+} ion as function of the magnetic field strength.

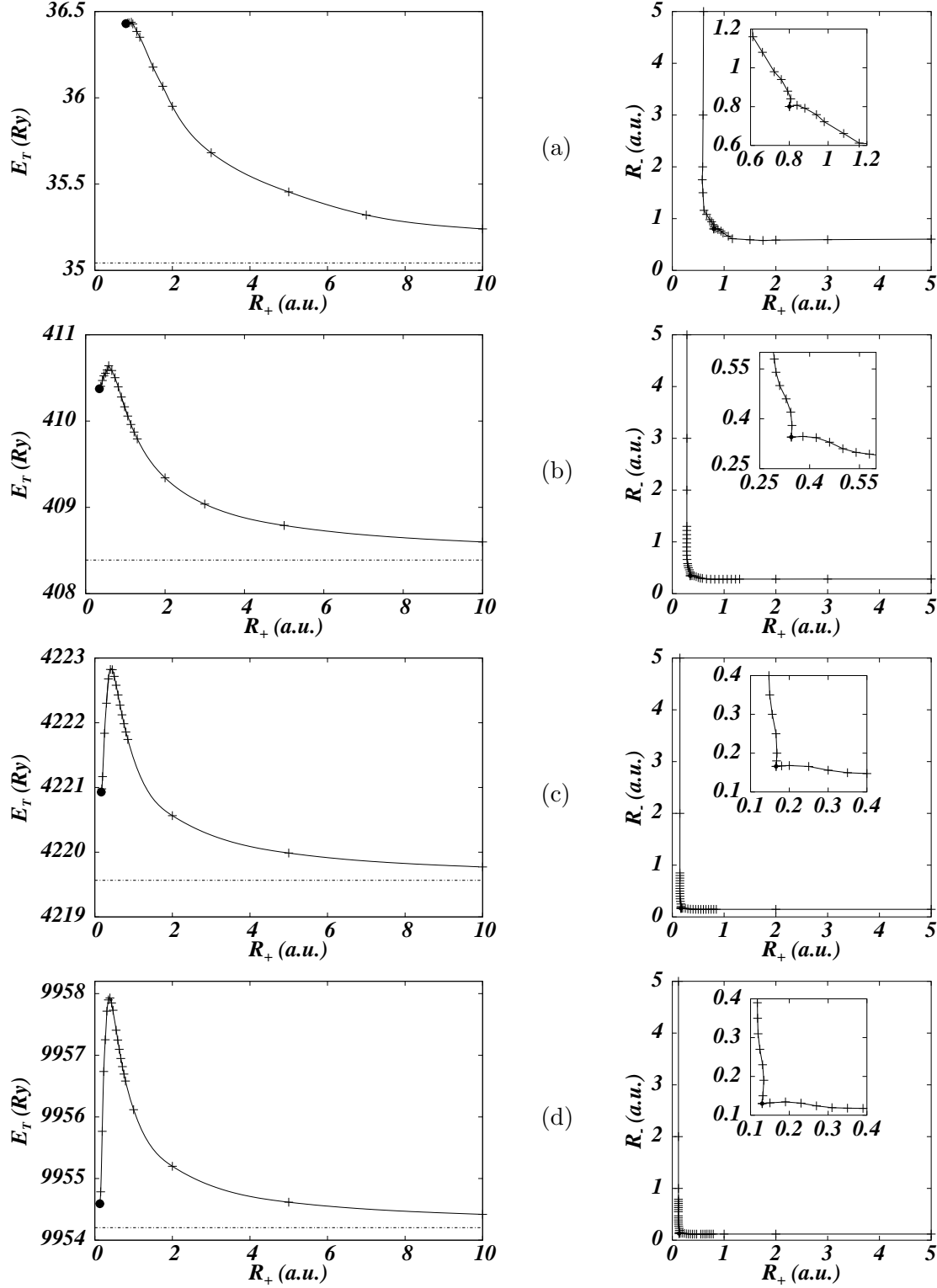


FIG. 4: Energy profiles along the valleys of minimal total energy for the H_3^{2+} ion as function of R_+ , R_- , and the corresponding paths in the plane (R_+, R_-) for different magnetic fields: (a) $B = 10^{11}$ G , (b) $B = 10^{12}$ G , (c) $B = 10^{13}$ G , (d) $B = 2.35 \times 10^{13}$ G, and (e) $B = 4.414 \times 10^{13}$ G. The position of the minimum is indicated by a bullet. The horizontal dashed line in the energy profile curve represents the energy of the H_2^+ ion.

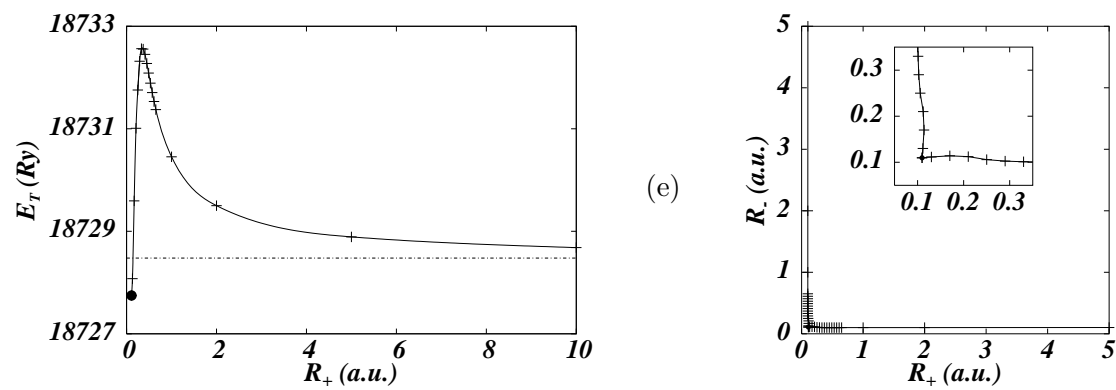


FIG. 4: Continuation

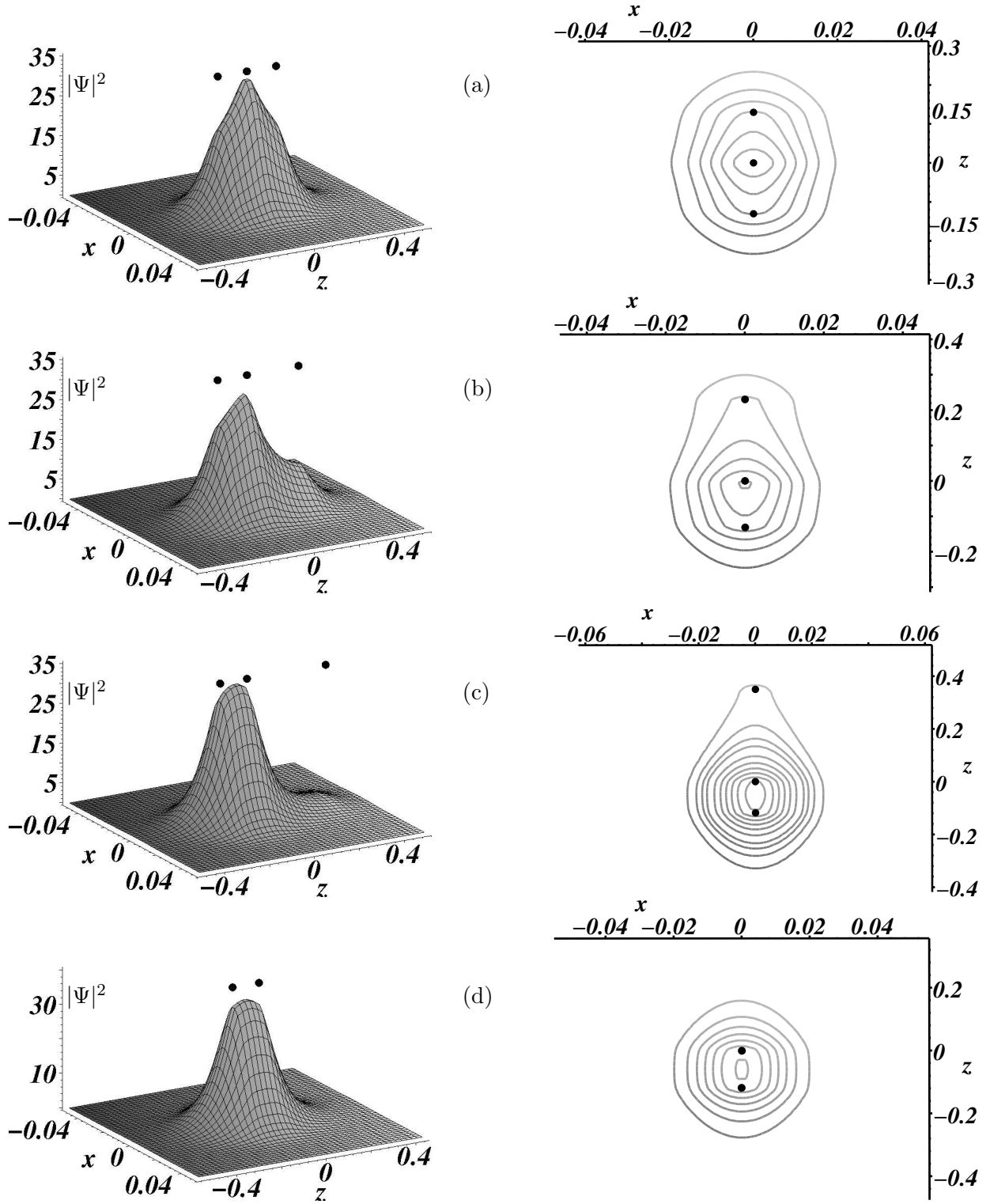


FIG. 5: Normalized electronic density distributions $\Psi^2(x, y = 0, z) / \int \Psi^2(x, y, z) d\vec{r}$ and their contours for the ground state $1\sigma_g$ of the H_3^{2+} ion along one of the valleys in a magnetic field $B = 10000$ a.u.: (a) $R_+ = R_{eq} = 0.13$ a.u., (b) $R_+ = 0.23$ a.u., (c) $R_+ = 0.35$ a.u. (near maximum, $R_+^{max} \simeq 0.36$ a.u.), (d) $R_+ = 5.0$ a.u. (third proton lies outside of the figure). The positions of the protons are marked by bullets. Vertical axis in the figures on the left is scaled to 1 : 1000.

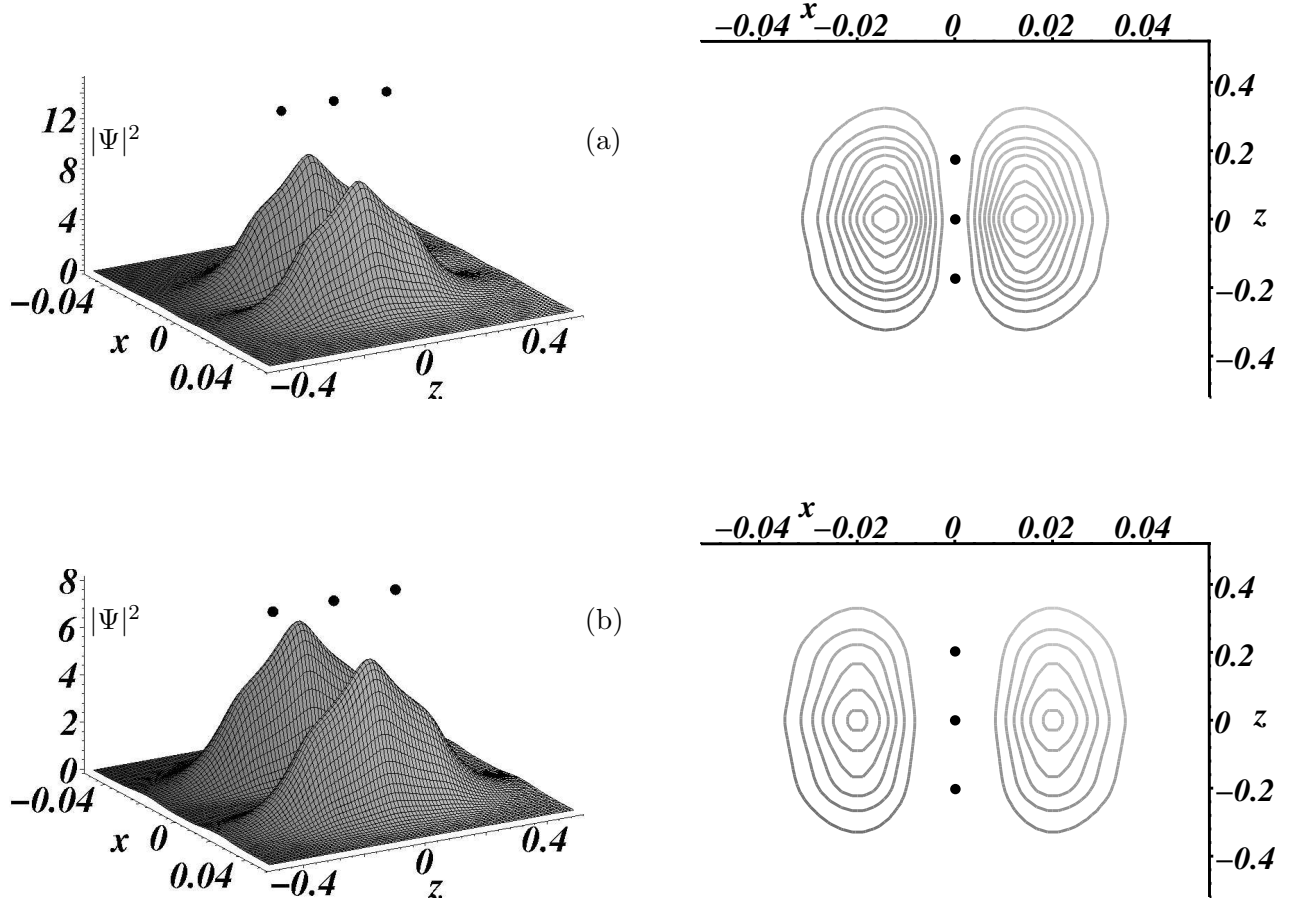


FIG. 6: Normalized electronic density distribution $\Psi^2(x, y = 0, z) / \int \Psi^2(x, y, z) d\vec{r}$ and the corresponding contours for the first two excited states (a) $1\pi_u$ and (b) $1\delta_g$ of the ion H_3^{2+} in a magnetic field $B = 10000$ a.u. The positions of the protons are marked by bullets. Vertical axis in the figures on the left is scaled to 1 : 1000.